Volume 1 | Number 1 | Jan 2013 | Pages 1–100

Nanoscale

www.rsc.org/nanoscale

ROYAL SOCIETY OF CHEMISTRY

ROYAL SOCIETY OF CHEMISTRY

www.rsc.org/nanoscale

Nanoscale

PAPER

Graphene Quantum Dots for the Inhibition of *β* Amyloid Aggregation

Yibiao Liu,[a,b] Li-Ping Xu,*[a,b] Wenhao Dai, [a,b] Haifeng Dong,[a,b] Yongqiang Wen,[a,b] and Xueji Zhang*[a,b]

The aggregation of A*β* peptides is a crucial factor of leading to Alzheimer's disease (AD). Inhibiting the A*β* peptides aggregation has become one of the most essential strategies to treat AD. In this work, an efficient and low-cytotoxicity inhibitor, graphene quantum dots (GQDs) are reported for application of inhibiting the aggregation of A*β* peptides. Compared to other carbon materials, low cytotoxicity and great biocompatibility of GQDs gives an advantage to the clinical research for AD. In addition, GQDs may cross the blood-brain barrier (BBB) because of the small size. It is believed that GQDs may be a therapeutic agents against AD. This work provides novel insight into the development of Alzheimer's drug.

Introduction

Alzheimer's disease (AD) is the most prevalent neurodegenerative disease. One of its important traits is cerebral extracellular amyloid plaques. [1, 2] The amyloid plaques are formed through the aggregation of *β*-amyloid (A*β*) peptide. A*β* peptide is an amphipathic polypeptide consisting of 39∼42 amino acids.[3] There are two principal variants of the A*β* peptide in humans——A*β*1-40 and A*β*1-42.[4] The former is more abundant and A*β*42 forms fibrils more rapidly.[4, 5] A*β*1-42 is the most common variant in human cerebrospinal fluid (CSF) and the aggregation of A*β*1-42 peptide is the main component of amyloid plaques.[6] The A*β*1-42 peptide contains two stretches of hydrophobic residues (16-20 and 30-40), which play an important role in the process of A*β*1-42 aggregation.[7] Furthermore, it also contains several charged amino acids residues (such as His, Glu, Asp and Lys).[8] The hydrophobic interaction and electrostatic interaction play a key role in the aggregation of A*β*1-42 peptide. Some studies have proved that the modifications of hydrophobic regions can accelerate or inhibit fibril formation and promote/induce the disassembly of A*β* fibrils.[9-12]

The aggregation of A*β* peptides is a critical factor leading to AD and the aggregates of A*β* peptides including soluble oligomers and mature fibrils are neurotoxic to brain cells.[1, 5, 13] Nowadays, obliterating the aggregates of A*β* peptides from the organs and prevention or interference of A*β* peptides aggregation are two major therapeutic strategies for AD. Hence, many A*β* peptides aggregation inhibitors were contemplated as potential drug candidates. Traditional inhibitors mainly consist of peptides or peptide mimetics[14-16] and small organic molecules[17-19]. However, their low blood-brain barrier permeability, the complexity of their synthesis,

the low in vivo stability and the low efficacy may hinder their applications.[1, 15, 20]

Considering the hydrophobicity of the central motif of A*β*1-42 peptides. Hydrophobic carbon nanomaterials have been widely applied to inhibit the A*β* peptides aggregation.[21-27] As a novel carbon nanomaterial, graphene has received much attention in materials science and biomedicine. Significant progress has been made for wide application of graphene or functionalization of graphene in cancer therapies,[28] drug delivery[29] and biosensing[30]. Graphene quantum dots (GQDs) are a single or few-layer graphene with a tiny size less than 100 nm. Due to its photoluminescence properties, edge effect, low cytotoxicity and great biocompatibility, GQDs are widely used in diverse fields of biological research, particular in nanobiomedicine[31] and cell imaging[32-34].
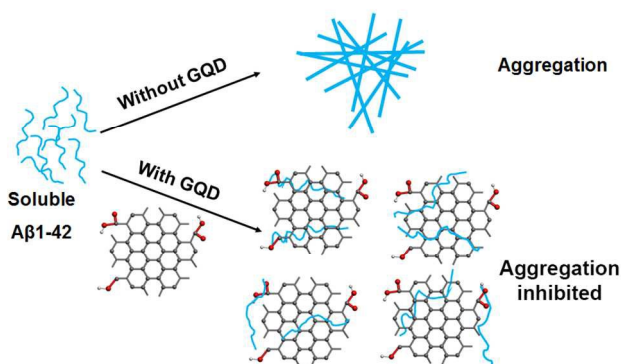

Fig. 1. Schematic representation of the GQDs used for inhibiting the aggregation of Aβ 1-42 peptides.

In this work, we synthetize the GQDs with average diameter of 8 nm and explore the effects of GQDs on the aggregation of Aβ peptides as shown in Fig. 1. The GQDs show the capability of efficiently inhibiting the aggregation of Aβ peptides. In addition, GQDs also rescue the cytotoxicity of Aβ oligomers. Considering these superiorities, GQDs may also be potential Aβ peptides inhibitors or Alzheimer's drug.

Experimental

Reagents

Aβ1-42 peptides were purchased from Beijing SBS Genctech Co. Ltd. Graphite nanoparticles were purchased from Alfa Aesar China. The GQDs were synthetized by hydrothermal methods according the reference[35]. All other reagents were of analytical reagent grade and commercially available. All solutions were prepared with ultrapure water in this work (Milli-Q, 18.2 MΩ cm).

The synthesis and characterization of GQDs

Firstly, graphene sheets (GSs, 0.05 g) were oxidized in concentrated H_2SO_4 (10 mL) and HNO_3 (30 mL) for 15 h under mild ultrasonication (500 W, 40 kHz). Secondly, the mixture was diluted with ultrapure water (250 mL) and filtered through a 0.22 μm microporous membrane to remove the acids. Purified oxidized GSs were re-dispersed in 75 mL ultrapure water/ethanol (1:1, v/v ratio). The suspension was transferred to a poly(tetrafluoroethylene) (Teflon)-lined autoclave (100 mL) and heated at 200 ℃ for 10 h. After cooling to room temperature, the resulting suspension was filtered through a 0.22 μm microporous membrane. The GQD3 was obtained in the filtrate. Adjusting the water/ethanol proportion, the GQD1(1:0, v/v ratio), GQD2(2:1, v/v ratio), GQD4(1:2, v//v ratio) and GQD5(0:1, v/v ratio) were obtained respectively. All the obtained GQDs were characterized by TEM (Hitachi 7000) and fluorescence spectrometer. And the surface charges of GQDs were measured by zeta potential measurement analyser (Nano-ZS90).

ThT fluorescence spectroscopy

The kinetics of Aβ1-42 peptides aggregation was monitored by using the dye ThT, the fluorescence of which was dependent on the formation of amyloid fibrils. Fluorescence measurements were carried out with a JASCO FP6500 spectrofluorometer. The fluorescence signal (excitation at 450 nm) was recorded between 460 and 600 nm; 10 nm slits were used for both emission and excitation measurements. The Aβ1-42 peptide concentration was 40 μM, and the ThT concentration was 10 μM. At different times, aliquots of the Aβ1-42 peptides solution were taken for fluorescence measurements.

Atomic Force Microscope (AFM) Characterization

The visualization of Aβ1-42 peptides aggregation with or without GQD at different times were performed using a Nanoscope Ⅲa Multimode AFM (Bruker Inc.) by tapping mode. 40 μM Aβ1–42 and 40 μM Aβ1–42 in the presence of GQDs were incubated for 7 days at 37 ℃. Briefly, aliquots of 20 μL of each sample were placed on a freshly cleaved substrate. After incubation for 10 min, the substrate was rinsed twice with water and dried before measurement. All tips (RTESP, 318-384 kHz) were got from Bruker Inc. The images presented here were non-filtered and composed by 512 × 512 pixels with scanning areas of 1 μm × 1 μm. All AFM images were processed using nanoscope analysis software.

Cell Toxicity Assays

Cell-toxicity assays: PC12 cells (rat pheochromocytoma, American Type Culture Collection) were cultured in RPMI-1640 supplemented with 10% fetal bovine serum in a humidified 5% CO_2 environment at 37 °C. Cells were plated at a density of 10 000 cells per well on 96-well plates in fresh medium. Aβ1-42 peptides (40 μM) that had been incubated with or without GQDs 6 days at 37 °C were added, and the PC12 cells were further incubated for 24 h at 37 °C. Cytotoxicity was measured by using a modified MTT assay kit (Promega). Absorbance values of formazan were determined at 490 nm with an automatic plate reader.

Results and Discussion
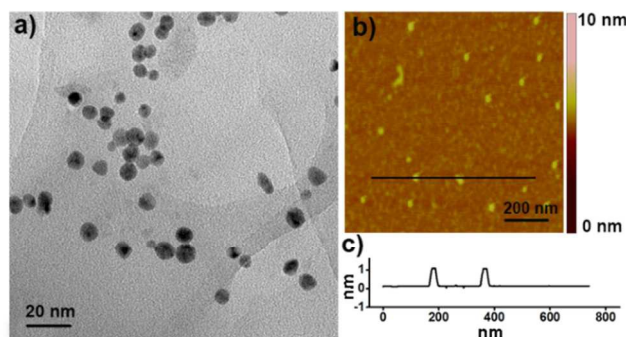
Synthesis and characterization of GQDs

Fig. 2. TEM a) and AFM b) characterization of GQD3. c) Section analysis of black line marked in b).

GQD3 were prepared by the addition of oxidized graphite sheets to water/ethanol (v/v, 1:1) solution and heating 10 h at 200 ℃. After cooling to room temperature, the resulting suspension was filtered through a 0.22 μm microporous membrane and the GQD3 were obtained in the separated solution. The obtained GQD3 were characterized using transmission electron microscopy (TEM). Fig. 2a shows the typical TEM image of GQD3. Quasi circular nanoparticles with average diameters of 8 nm were clearly observed (Fig. 2a). The AFM images of GQD3 were shown in Fig. 2b and 2c, the average height of GQD3 were less than 1.3 nm. These results indicated that the GQDs were single layers. By changing the proportions of water/ethanol, the other four GQDs were obtained. All the five GQDs have similar sizes as indicated in Fig. S2 and Fig. S3. Furthermore, the charges of GQDs were measured by zeta

potential instrument. As shown in Fig. 4a, all the five GQDs are negative and the surface potential of GQDs decreases successively from GQD1 to GQD5. In the next discussion, GQDs defaults to GQD3 unless otherwise specified.

The effect of GQDs on the process of Aβ1-42 peptides fibrillation

After synthetizing the GQDs, the inhibition activity of the especial carbon materials in Aβ peptides aggregation was investigated. The effect of GQDs on the assembly of Aβ1-42 peptides was employed by thioflavin T (ThT) fluorescence assay. ThT is an extrinsic fluorescent dye and can combine with amyloid fibrils; its fluorescence intensity increases with the augment of conjugates[36]. The fibrillation process was monitored by measuring the fluorescence intensity of ThT at 490 nm upon excitation at 450 nm. As shown in Fig. 3A, the process of Aβ1-42 peptides aggregation illustrates three stages of a typical protein fibrillation, that is, lag phase, elongation phase, and steady state. In the lag phase, the monomeric Aβ aggregated into small clusters. The ThT fluorescence intensity increased slowly for the first few hours when fresh Aβ1-42 peptide alone was incubated at 37℃. Previous studies also showed that the lag phase was a rate-limiting step[37-39].
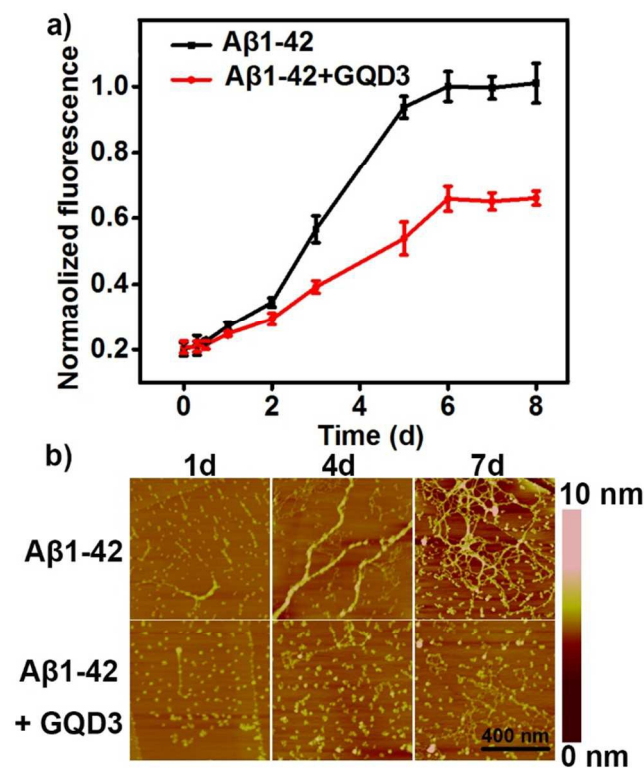

Fig. 3. Inhibition of Aβ1-42 peptides aggregation by GQD3. (a) The kinetics of Aβ1-42 aggregation as monitored by the thioflavin T fluorescence in the absence of GQD3 or in the presence of GQD3. (b) AFM image of a control sample containing Aβ1-42 in 10 mM PBS buffer (pH 7.4) with or without GQD3 after incubation at 37 °C for different incubation times. (AFM：Tapping mode, size: 1 μm×1 μm.)

As the end of lag phase, a lot of clusters aggregated into amyloid fibrils and the ThT fluorescence intensity started to rise rapidly (Fig. 3a, the black line). However, the value of ThT fluorescence significantly decreased in the presence of GQDs. (Fig. 3A, the red line). It was obvious that the accumulation rate of Aβ1-42 peptides slowed down observably in the presence of GQDs. These results indicated that the formation of amyloid fibrils was suppressed by GQDs. In order to verify further the inhibitory effect of GQDs, we also investigated the morphology of Aβ1-42 peptide in the presence or absence of GQDs at different incubation times by AFM. A 40 μM solution of Aβ1-42 was incubated with and without GQDs in PBS buffer (10 mM) at 37℃ for several days. Aβ1-42 formed a typical structure for amyloid fibrils (Fig. 3b, the top line). In the presence of GQDs, no fibrils were observed (Fig. 3b, the bottom line). The AFM data further supported the results with ThT fluorescence assay and indicate that GQDs can inhibit amyloid fibril formation.

The effect of GQDs with different charges on the aggregation of Aβ1-42 peptide was monitored by ThT fluorescence assay. The results demonstrate that the inhibiting affectivity of GQDs on Aβ1-42 peptides aggregation increases obviously with the decrease of the surface negative charge (Fig. 4b). Furthermore, we investigated the morphology of Aβ1-42 peptides aggregates by AFM. As can be seen from the Fig. 4c, we found that the Aβ1-42 peptides alone can aggregate into mature fibrils. In the presence of GQDs, the fibrils were disaggregated and only some clusters were observed. Moreover, the aggregation level of Aβ1-42 peptides with five kinds of GQDs treatment respectively lowered with the decrease of surface negative charge. These results further proved that the inhibiting affectivity of GQDs enhanced with the decrease of the surface negative charge.

According to the previous reports,[40, 41] hydrophobic interactions and electrostatic interactions are the two most important factors of inhibiting the Aβ1-42 peptides aggregation. In recent years, various carbon materials[25-27] including fullerene, carbon nanotubes and graphene oxide were applied to inhibit the Aβ1-42 peptides aggregation. They found that hydrophobic interactions play an important role in the process of interaction between carbon materials and Aβ1-42 peptides. In this work, as one of carbon nanomaterials, GQDs were also proved to inhibit the Aβ1-42 peptides aggregation. The GQDs may also specifically binds to the central hydrophobic motif of Aβ1-42 peptides. Moreover, the negative charges of GQDs may interact with positively charged His residues of Aβ1-42 peptides. In the previous studies, Tjernberg et al.[40] found that the electrostatic interactions between imidazolium groups on His residues and carboxylate groups on Asp and Glu residues play an important role in the Aβ1-42 peptides aggregation. Morteza Mahmoudi et al. also found that the negative superparamagnetic iron oxide nanoparticles (SPIONs) can delay or inhibit the Aβ1-42 peptide aggregation[41]. In this work, the inhibiting affectivity of GQDs decreases with the increase of the surface negative charge. The electrostatic interactions interfere the hydrophobic interactions between the inhibitors and Aβ1-42 peptides. Based on the analysis above, we conclude

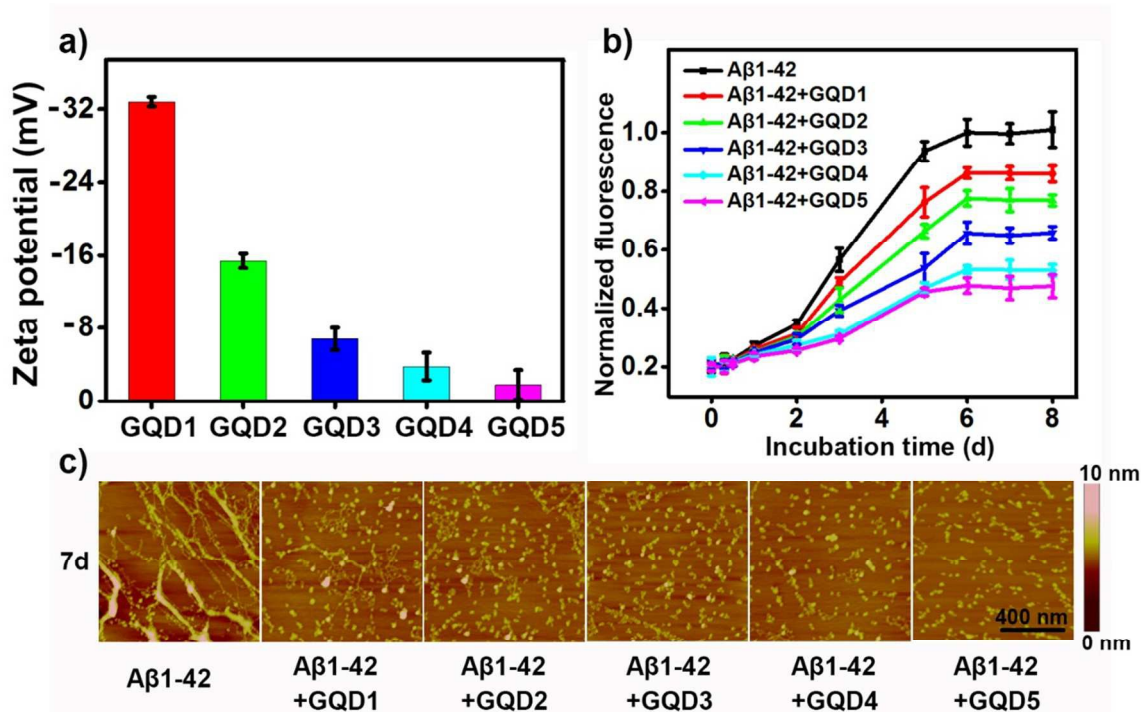that hydrophobic interactions may play more dominant roles in the process of inhibiting the aggregation.

Fig. 4. Inhibition of Aβ1-42 peptides aggregation by GQDs with different charge. a) The zeta potential of GQDs with different charge. b) The kinetics of Aβ1-42 aggregation as monitored by the thioflavin T fluorescence in the absence or presence of GQDs with different charge. c) AFM image of a control sample containing Aβ1-42 in 10 mM PBS buffer (pH 7.4) with or without GQDs after incubation 7 days at 37 ° C. (AFM：Tapping mode, size: 1 μm×1 μm.)

GQDs rescue Aβ-induced cytotoxicity

The ability of GQDs to inhibit Aβ1-42 peptides assembly suggested that they might be useful in blocking Aβ-mediated cellular toxicity. Moreover, Aβ-induced cytotoxicity is an important factor to lead to AD. To explore the effect of GQDs on Aβ1-42-mediated cellular toxicity, we used PC12 cells by employing 3-(4, 5-dimethylthiazol-2-yl)-2, 5-diphenyltetrazolium bromide (MTT) assay to explore the cellular metabolism. As can be seen in Fig. 5, Aβ1-42 peptides alone bring about a decrease of 41% in cellular reduction of MTT (lane 2). Treatment of the cells with Aβ1-42 peptides in the presence of GQDs increases the survival of the cells to about 80% (Fig. 5, lane 3). As depicted by the lane 4 in Fig. 5, GQDs alone decrease the survival of cells to 92%, which indicates that GQDs themselves are nearly nontoxic under the same conditions. As expected, GQDs are very effective to inhibit the aggregation of Aβ1-42 peptide evidenced by ThT fluorescence assay analysis and AFM. Previous studies have demonstrated that most carbon materials such as carbon nanotube, fullerene, larger size graphene are too toxic to envision their clinical use as anti-AD drugs though these carbon materials all can inhibit the aggregation of Aβ peptides. [25, 27, 42-44]

However, GQDs are good to solve the problem of other carbon materials-induced cytotoxicity and make it possible for the clinical trial. Furthermore, the inhibiting affectivity of GQDs is also excellent. The mean inhibitory constant (IC_{50}) were obtained by Th

T fluorescence intensity as shown in Fig. S1. In addition, the reported IC_{50} values were normalized to the Aβ peptides concentration of 20 μM.[21, 45-48] As can be seen in table S1, GQDs shows one of the lowest IC_{50} values among the six inhibitors for Aβ peptides aggregation. It is expected that this study will provide a better nanomaterials as a therapeutic drug for AD.
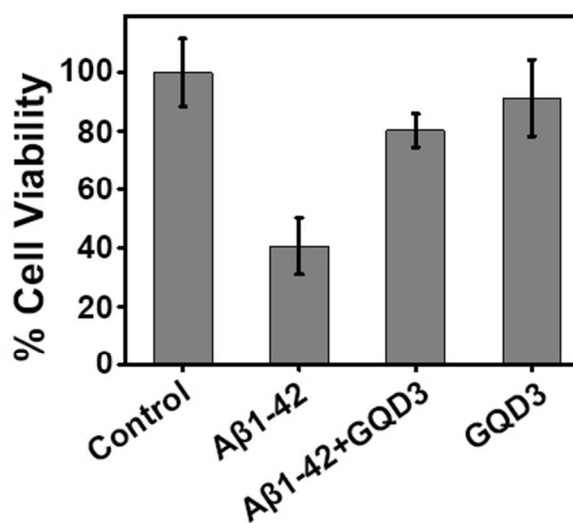

Fig. 5. The effect of GQDs on the cell toxicity of Aβ1-42 peptide. Cell viability was determined using MTT method.

Conclusions

In this work, GQDs are demonstrated to inhibit efficiently the aggregation of Aβ1-42 peptides as a low-cytotoxicity inhibitor. Here GQDs with average diameters of 8 nm were synthesized and exhibited excellent inhibiting effect on the aggregation of Aβ1-42 peptides. Cytotoxicity experiment has proved that GQDs are almost non-toxic to PC-12 cells. Compared to other carbon material, GQDs have excellent photoluminescence properties, low cytotoxicity and great biocompatibility, which make it possible for clinical application. As far as we know, it has not been reported previously that GQDs can inhibit Aβ peptides aggregation and recue the Aβ-induced cytotoxicity. It can be anticipated that this study will significantly promote the development of therapeutic drug for AD.

Acknowledgements

Notes and references

^{a} Research Center for Bioengineering and Sensing Technology, University of Science & Technology Beijing, Beijing 100083, P.R. China. Fax: 86-10-82375840; Tel: 86-10-82375840; E-mail: xuliping@ustb.edu.cn; zhangxueji@ustb.edu.cn.
^{b} School of Chemistry and Biological Engineering, University of Science and Technology Beijing, Beijing, 100083, P.R. China.
† Electronic Supplementary Information (ESI) available: Dose-dependent inhibition of Aβ1-42 fibrillization by GQDs; The photoluminescence spectra of all five GQDs with different charges in water/ethanol; TEM images of other four GQDs with different charges. See DOI: 10.1039/b000000x/

1.   J. Hardy and D. J. Selkoe, *Science*, 2002, **297**, 353-356.
2.   M. Goedert and M. G. Spillantini, *Science*, 2006, **314**, 777-781.
3.   D. M. Walsh, D. M. Hartley, Y. Kusumoto, Y. Fezoui, M. M. Condron, A. Lomakin, G. B. Benedek, D. J. Selkoe and D. B. Teplow, *J. Biol. Chem.*, 1999, **274**, 25945-25952.
4.   D. J. Selkoe, *Physiol. Rev.*, 2001, **81**, 741-766.
5.   P. T. Lansbury and H. A. Lashuel, *Nature*, 2006, **443**, 774-779.
6.   A. E. Roher, J. D. Lowenson, S. Clarke, A. S. Woods, R. J. Cotter, E. Gowing and M. J. Ball, *Proc. Natl. Acad. Sci. U.S.A.*, 1993, **90**, 10836-10840.
7.   L.P. Xu, Y. B. Liu and X. J. Zhang, *Nanoscale*, 2011, **3**, 4901-4915.
8.   M. Guo, P. M. Gorman, M. Rico, A. Chakrabartty and D. V. Laurents, *FEBS Lett.*, 2005, **579**, 3574-3578.
9.   R. T. Liu, C. McAllister, Y. Lyubchenko and M. R. Sierks, *J. Neurosci. Res.*, 2004, **75**, 162-171.
10. T. L. Lowe, A. Strzelec, L. L. Kiessling and R. M. Murphy, *Biochemistry*, 2001, **40**, 7882-7889.
11. C. K. Bett, J. N. Ngunjiri, W. K. Serem, K. R. Fontenot, R. P. Hammer, R. L. McCarley and J. C. Garno, *ACS Chem. Neurosci.*, 2010, **1**, 608-626.
12. Y. B. Liu, L. P. Xu, H. Z. Yu, Y. Q. Wen and X. J. Zhang, *Chem. Phys. Lett.*, 2014, **608**, 201-206.
13. G. Yamin, K. Ono, M. Inayathullah and D. B. Teplow, *Curr. Pharm. Des.*, 2008, **14**, 3231-3246.
14. A. Frydman-Marom, M. Rechter, I. Shefler, Y. Bram, D. E. Shalev and E. Gazit, *Angew. Chem.*, 2009, **121**, 2015-2020.
15. T. Takahashi and H. Mihara, *Acc. Chem. Res.*, 2008, **41**, 1309-1318.
16. C. Soto, E. M. Sigurdsson, L. Morelli, R. A. Kumar, E. M. Castaño and B. Frangione, *Nat. Med.*,1998, **4**, 822-826.
17. D. E. Ehrnhoefer, J. Bieschke, A. Boeddrich, M. Herbst, L. Masino, R. Lurz, S. Engemann, A. Pastore and E. E. Wanker, *Nat. Struct. Mol. Biol.*, 2008, **15**, 558-566.
18. F. Yang, G. P. Lim, A. N. Begum, O. J. Ubeda, M. R. Simmons, S. S. Ambegaokar, P. P. Chen, R. Kayed, C. G. Glabe, S. A. Frautschy and G. M. Cole, *J. Biol. Chem.*, 2005, **280**, 5892-5901.
19. K. Barbara, M. Cortijo-Arellano, J. Cladera, M. Jean-Pierre, C. Anne-Marie and M. Bryszewska., *Biochem. Bioph. Res. Co.*, 2007, **364**, 20-25.
20. J. F. Poduslo, G. L. Curran and C. T. Berg, *Proc. Natl. Acad. Sci. USA*, 1994, **91**, 5705-5709.
21. J. E. Kim and M. Lee. *Biochem. Bioph. Res. Co.*, 2003, **303**, 576-579.
22. A. G. Bobylev, A. B. Kornev, L. G. Bobyleva, M. D. Shpagina, I. S. Fadeeva, R. S. Fadeev, D. G. Deryabin, J. Balzarini, P. A. Troshin and Z. A. Podlubnaya, *Org. Biomol. Chem.*, 2011, **9**, 5714-5719.
23. H. Y. Li, Y. Luo, P. Derreumaux and G. H. Wei, *Biophys. J.*, 2011, **101**, 2267-2276.
24. Z. M. Fu, Y. Luo, P. Derreumaux and G. H. Wei, *Biophys. J.*, 2009, **97**, 1795-1803.
25. M. Mahmoudi, O. Akhavan, M. Ghavami, F. Rezaee and S. M. A. Ghiasi, *Nanoscale*, 2012, **4**, 7322-7325.
26. J. Luo, S. K. T. S., Wärmländer, C. H. Yu, K. Muhammad, A. Gräslund and J. P. Abrahams, *Nanoscale*, 2014, **6**, 6720-6726.
27. L. Xie, Y. Luo, D. Lin, W. Xi, X. Yang and G. H. Wei, *Nanoscale*, 2014, **6**, 9752-9762.
28. O. Akhavan, E. Ghaderi, S. Aghayee, Y. Fereydooni and A. Talebi, *J. Mater. Chem.*, 2012, **22**, 13773-13781.
29. Z. Liu, J. T. Robinson, X. Sun and H. Dai, *J. Am. Chem. Soc.*, 2008, **130**, 10876-10877.
30. O. Akhavan, E. Ghaderi and R. Rahighi, *ACS Nano*, 2012, **6**, 2904-2916.
31. H. Tao, K. Yang, Z. Ma, J. Wan, Y. Zhang, Z. Kang and Z Liu, Small, 2012, **8**, 281-290.
32. S. J. Zhu, J. H. Zhang, C. Y. Qiao, S. J. Tang, Y. F. Li, W. J. Yuan, B. Li, L. Tian, F. Liu, R. Hu, H. Gao, H. Wei and H. Zhang, *Chem. Commun.*, 2011, **47**, 6858-6860.

33. Y. Liu and P. Wu, *ACS Appl. Mater. Interfaces*, 2013, **5**, 3362-3369.

34. J. Peng, W. Gao, B. K. Gupta, Z. Liu, R. Romero-Aburto, L. Ge, L. Song, L. B. Alemany, X. Zhan, G. Gao, S. A. Vithayathil, B. A. Kaipparettu, A. A. Marti, T. Hayashi, J. J. Zhu, P. M. Ajayan, *Nano Lett.*, 2012, **12,** 844-849.

35. D. Y. Pan, J. C. Zhang, Z. Li and M. H. Wu, *Adv. Mater.*, 2010, **22**, 734-738.

36. H. Levine, *Protein Sci.*, 1993, **2**, 404-410.

37. D. M. Walsh, A. Lomakin, G. B. Benedek, M. M. Condron and D. B. Teplow, *J. Biol. Chem.*, 1997, **272**, 22364-22372.

38. J. T. Jarrett, E. P. Berger and P. T. Lansbury, *Biochemistry*, 1993, **32**, 4693-4697.

39. V. Rangachari, B. D. Moore, D. K. Reed, L. K. Sonoda, A. W. Bridges, E. Conboy, D. Hartigan and T. L. Rosenberry, 2007, *Biochemistry*, **46**, 12451-12462.

40. L. O. Tjernberg, D. J. E. Callaway, A. Tjernberg,, S. Hahne, C. Lilliehöök,, L. Terenius,, J. Thyberg and C. Nordstedt, *J. Biol. Chem.*, 1999, **274**, 12619-12625.

41. M. Mahmoudi, F. Quinlan-Pluck, M. P. Monopoli, S. Sheibani, H. Vali, K. A. Dawson and I. Lynch, *ACS Chem. Neurosci.*, 2013, **4**, 475-485.

42. R. H. Hurt, M. Monthioux and A. Kane, *Carbon*, 2006, **44**, 1028-1033.

43. A. Nel, T. Xia, L. Mädler and N. Li, *Science*, 2006, **311**, 622-627.

44. S. K. Smart, A. I. Cassady, G. Q. Lu and D. J. Martin, *Carbon*, 2006, **44**, 1034-1047.

45. D. R. Howlett, A.E. Perry, F. Godfrey, J. E. Swatton, K. H. Jennings, C. Spitzfaden, H. Wadsworth, S. J. Wood and R. E. Markwell, *Biochem. J.*, 1999, **340**, 283-289.

46. S. J. Wood, L. MacKenizies, B. Maleeff, M. R. Hurle and R. Wetzel, *J. Biol. Chem.*, 1996, **271**, 4086-4092.

47. B. Poeggeler, L. Miravalle, M. G. Zagorski, T. Wisniewski, Y. J. Chyan, Y. Zhang, H. Shao, T. Bryant-Thomas, R. Vidal, B. Frangione, J. Ghiso and M. A. Pappolla, *Biochemistry*, 2001, **40**, 14995-15001.

48. J. Geng, M. Li, J. Ren, E. Wang and X. G. Qu, *Angew. Chem. Int. Ed.*, 2011, **50**, 4184-4188.